minerals

MDPI

Article

Three-Dimensional Mineralization Prediction Using the Information Value Method: A Case Study of the Bainiuchang Ag Polymetallic Deposit, Southwest China

Fuju Jia [1], Guolong Zheng [2,*], Guangzhi Meng [2], Long Jian [3], He Chang [1,*], Ping Pan [3], Jianguo Gao [1], Zhixiao Wu [1] and Ceting Yang [1]

[1] College of Land Resources and Engineering, Kunming University of Science and Technology, Kunming 650093, China
[2] No. 306 Geological Party of Yunnan Nonferrous Geological Bureau, Kunming 650217, China
[3] Kunming Metallurgy College, Kunming 650033, China
* Correspondence: gl_zheng2022@163.com (G.Z.); hechang@kust.edu.cn (H.C.)

Abstract

Three-dimensional geological modeling combined with the information value method offers a powerful approach for predicting mineralization in complex geological settings. This study applies these techniques to the Bainiuchang Ag polymetallic deposit in Southwest China. We constructed a detailed 3D geological model to identify key geological factors influencing mineralization, such as the F_3 fault, secondary faults, and the middle Cambrian Tianpeng Formation. Using the information value method, we evaluated the mineralization potential of each unit in the study area. Receiver operating characteristic (ROC) curves and fractal analysis were employed to determine an optimal threshold (information value > 2.6) for delineating high-potential exploration targets. Our results identified three priority targets (A1, A2, and A3), demonstrating the effectiveness of integrating 3D modeling with probabilistic mineral prospectivity mapping. This approach provides a robust framework for deep and peripheral exploration in structurally complex deposits, offering valuable insights for future mineral exploration efforts.

Keywords: deposit model; 3D information value method; mineralization prediction; Bainiuchang Ag polymetallic deposit; southwest China

check for updates

Academic Editors: Giovanni Grieco, David Lentz, Jia-Xi Zhou, Jaroslav Dostal and Xavier Emery

Received: 6 June 2025
Revised: 22 July 2025
Accepted: 24 July 2025
Published: 25 July 2025

Citation: Jia, F.; Zheng, G.; Meng, G.; Jian, L.; Chang, H.; Pan, P.; Gao, J.; Wu, Z.; Yang, C. Three-Dimensional Mineralization Prediction Using the Information Value Method: A Case Study of the Bainiuchang Ag Polymetallic Deposit, Southwest China. *Minerals* **2025**, *15*, 783. https://doi.org/10.3390/min15080783

Copyright: © 2025 by the authors. Licensee MDPI, Basel, Switzerland. This article is an open access article distributed under the terms and conditions of the Creative Commons Attribution (CC BY) license (https://creativecommons.org/licenses/by/4.0/).

1. Introduction

Three-dimensional (3D) geological modeling has been widely applied in the mining industry to visualize and interpret complex geological structures and predict the spatial distribution of mineralization [1–4]. This technique allows the integration of diverse datasets, including geological maps, borehole data, and geophysical surveys, into a coherent 3D framework. By constructing detailed 3D models, geologists can better understand the relationships between geological structures and mineralization, and identify potential exploration targets more accurately [5–7]. For example, 3D geological modeling of the Jiaojia Au deposit in China was used to reconstruct the deep 3D geometry of detachment faults in the Jiaodong Au province using a Bayesian approach, integrating multi-source information and geological constraints to estimate the uncertainty, validate models using drilling data, and identify potential Au exploration targets [8].

The information value method is another important tool for mineralization prediction, and has been widely used to evaluate the contribution of different geological factors

to the occurrence of mineral deposits [9,10]. This method quantifies the relationship between geological features and known mineral occurrences, allowing calculation of the information value for each factor and the identification of areas with a high mineralization potential. Although the information value method has been widely applied in 2D mineral prospectivity mapping, few studies have attempted to undertake 3D quantitative mineral prospectivity modeling [11–13].

The 3D information value method offers a more realistic simulation of geological elements than the 2D information value method by incorporating the third dimension, which is crucial for accurately representing the spatial distribution and complexity of mineral deposits. This enhanced realism enables better quantification of the geological factors influencing mineralization. Compared to machine learning methods, the 3D information value method is transparent and clearly defines relationships between variables. This transparency enhances the interpretability of results, providing clear insights into the geological factors influencing predictions. Moreover, the results are traceable, allowing for step-by-step verification and error correction.

In this study, we focused on the Bainiuchang Ag polymetallic deposit, which has complex geological structures and significant mineralization potential. A detailed geological model of the deposit was constructed, incorporating strata, faults, igneous rocks, and ore bodies. The 3D information value method was used to evaluate the controls of these geological elements on the spatial distribution of mineralization. Specifically, the total information value of each cell within the study area was calculated, and the boundaries of information value anomalies were delineated. Using this approach, three 3D prospecting targets were identified, thereby verifying the feasibility and effectiveness of the 3D information value method applied to this deposit. This study aimed to provide a comprehensive understanding of the geological controls on mineralization in the Bainiuchang deposit and develop a practical approach for identifying potential exploration targets in similar geological settings.

2. Geological Background and Ore Deposit Model

2.1. Geological Background

The Bainiuchang Ag polymetallic deposit is located between the Cathaysia, Yangtze, and Indochina blocks (Figure 1). The area has been affected by multiple phases of tectonism and magmatism, and had excellent conditions for mineralization. The deposit contains 6.47 thousand tons of Ag, 1.72 million tons of Zn, 1.10 million tons of Pb, and abundant Cu, Sn, and In [14,15].

The main strata in the mining area are Devonian (D) and Cambrian (∈) in age. The Devonian rocks are mainly mudstone, siltstone, and limestone (Figure 2a). The Cambrian strata comprise interbedded limestone, mudstone, and siltstone, and the dominant ore-hosting strata are in the middle Cambrian Tianpeng Formation ($\in_2$t). There are two sets of NW–SE-trending normal faults in the ore district. F_3 is the main fault (dip to the SW at 9°–37°) and secondary, steeply dipping faults occur in the hanging wall of F_3 (including F_4–F_9; dip to the SW at 40°–75°). The main ore bodies occur in the footwall of F_3, which is the ore-controlling fault of the deposit (Figure 2b).

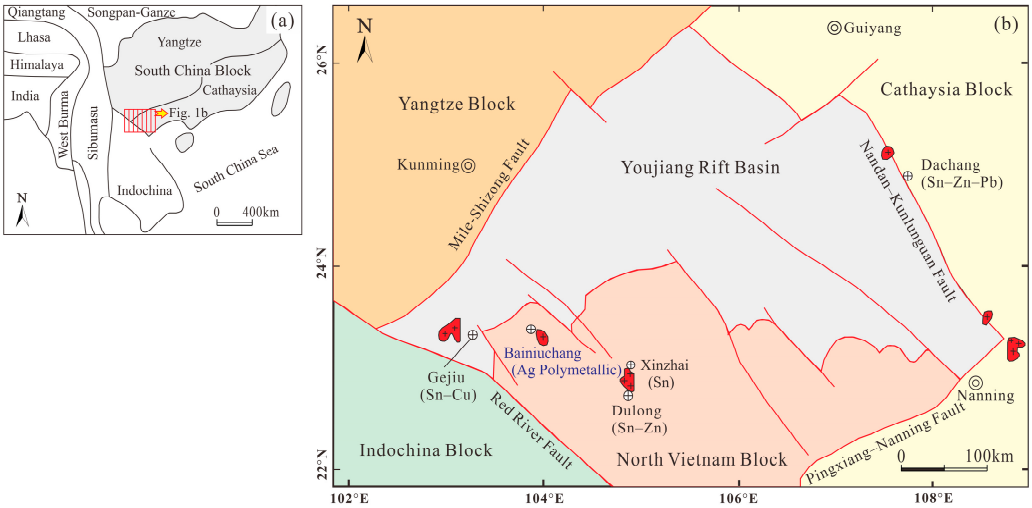


Figure 1. Tectonic setting and regional geological map of the Bainiuchang deposit. (**a**) Simplified map of eastern Asia showing major tectonic units (based on [16]). (**b**) Regional geological map (based on [17]).

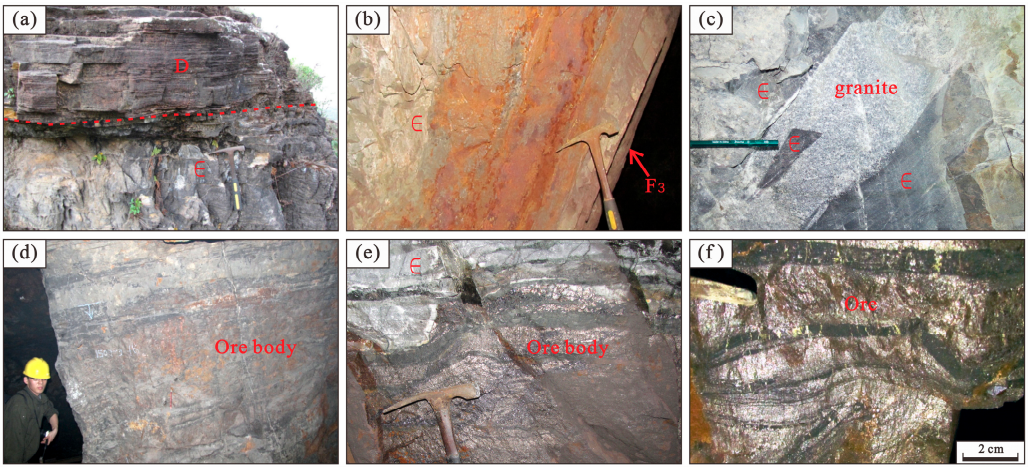


Figure 2. Strata, fault, granite, and ore body at the Bainiuchang ore deposit. (**a**) The Devonian (D) and Cambrian (∈) formations are in parallel unconformity contact. (**b**) The fault plane of the F_3 fault is consistent with the strata. (**c**) The granite intrudes into the Cambrian limestone (∈) in the form of dikes. (**d**) Massive polymetallic sulfide ore body. (**e**) The contact interface between the ore body and the Cambrian limestone (∈) is distinct. (**f**) Microfolds in the polymetallic sulfide ore.

Three biotite monzogranitic porphyries are exposed in the southern part of the mining area, and there is concealed biotite monzogranite in the southeastern part of the mining area (Figure 2c). Isotopic dating of the granitic porphyries and monzogranites has yielded Late Cretaceous ages, with the monzogranite having a zircon U–Pb age of 85.26 ± 0.54 Ma [14].

Over 70 ore bodies occur as stratiform to lenticular zones, with >75% of the resources concentrated in the V_1 ore body (along-strike length = 4.8 km, along-dip extent = 2.5 km, average thickness = 5.5 m). The main ore minerals are galena, sphalerite, chalcopyrite, cassiterite, miargyrite, freibergite, and stromeyerite. The main gangue minerals are calcite, dolomite, and quartz (Figure 2d–f).

2.2. Ore Deposit Model

The Bainiuchang ore deposit was modeled within a spatial framework that spans surface elevations from 2278 to 1712 m, extending 6.16 km from north to south and 7.00 km from east to west. Geological boundaries were delineated using data from extensive geological surveys and prospecting engineering efforts, which were integrated into the

3Dmine software. The dataset incorporated over 50 km of mining tunnels, 150 drill holes (with a cumulative length exceeding 80,000 m), and 35 geological cross-section diagrams. Based on the established boundaries, the model of each geological factor was appropriately extrapolated to provide a comprehensive representation of the deposit.

The modeled strata include the middle Cambrian Dayakou ($\in_2$d), Tianpeng ($\in_2$t), and Longha ($\in_2$l) formations, and a Devonian (D) formation. The modeled faults include the main fault (F_3) and secondary faults (F_4–F_9). The modeled igneous rocks include the granite and granitic porphyry. The ore body models were established with boundary grades of 40 g/t Ag, 0.30 wt.% Pb, 0.50 wt.% Zn, 0.20 wt.% Sn, and 0.30 wt.% Cu.

The cell is the carrier of mineralization information and the basic unit for mineralization prediction. Excessive refinement of cell divisions has been shown to artificially fragment geological phenomena and significantly complicate the processing of large datasets. On the other hand, overly coarse cell divisions can undermine the reliability of the morphological distribution of ore-bearing units. To address these challenges, the following factors were taken into account: the stratigraphy, geological structure, granite distribution, and the occurrence and scale of ore bodies within the deposit model, as well as the computational capacity for data processing. Based on these considerations, a 20 m × 20 m × 20 m cubic block was selected as the optimal unit for analysis. Based on a 20 × 20 × 20 m cube as the unit block, the modeling area contains 10,833,067 cells of which 25,735 are ore-bearing cells (Figure 3).

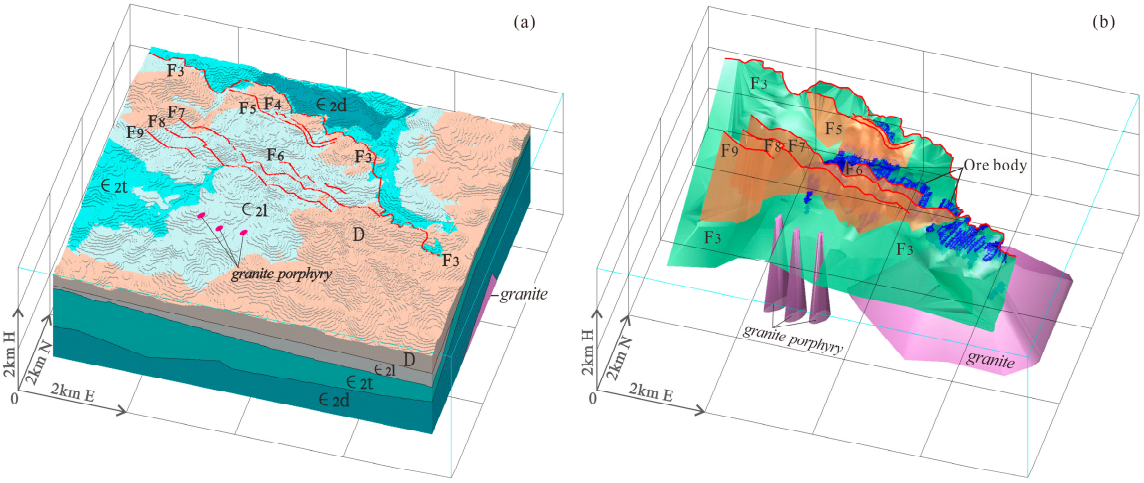


Figure 3. Geological model of the Bainiuchang ore deposit. (**a**) Geological model of the strata, granite, and granitic porphyry. (**b**) Model of the faults and ore bodies. $\in_2$d—middle Cambrian Dayakou Formation; $\in_2$t—middle Cambrian Tianpeng Formation; $\in_2$l—middle Cambrian Longha Formation; D—Devonian formation; F_3—F_3 fault; F_4–F_9—secondary faults.

3. Prediction Method and Variable Selection

We carried out a field geological survey of the Bainiuchang mine area and collected and collated data from previous mineral exploration and exploitation. A detailed geological model was constructed, integrating strata, faults, igneous rocks, and ore bodies. The 3D information value method was then applied to identify 3D prospecting targets. An overview flowchart is presented in Figure 4.

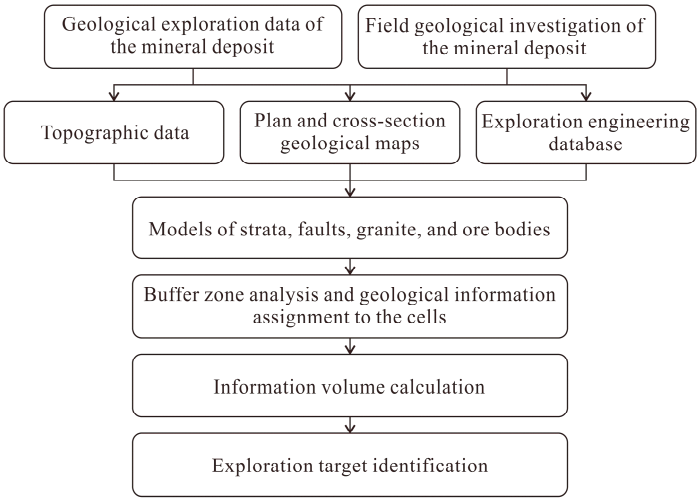


Figure 4. The methodological flowchart implemented in this study.

3.1. Information Value Method

The information value method is a powerful tool for summarizing and analyzing relevant information, and is particularly useful for mineralization prediction and natural hazard prediction [18–21]. The method was employed to summarize the relevant information for mineralization prediction, then calculate and analyze the amount of information pertaining to geological factors [22,23]. The obtained information values can be used as indexes to evaluate whether the relationship between each geological factor and the research object is close, and to assess the extent to which the geological factors affect the exploration and thereby predict the location of the favorable mineralization area(s). The equation for calculating the information values is

$$I(xi,\ H) = lg\frac{(Ni/N)}{(Si/S)} \tag{1}$$

where *I(xi, H)* represents the information value provided by the evaluation geological factor *xi* for mineralization *H*. *Ni* is the number of ore-bearing cells in the buffer zone, *N* is the total number of ore-bearing cells in the study area, *Si* is the total number of cells in the buffer zone, and *S* is the total number of cells in the study area. Based on the information value theory, *I(xi, H)* can be positive, negative, or zero, indicating there is a positive, negative, or no association, respectively, between the known ore occurrences and buffer zone of each geological factor.

The positive information values were selected and summed to obtain the information value of the evaluation cells in the study area, which is expressed as follows:

$$Ii = \sum_{i=1}^{n} I(xi, H) = \sum_{i=1}^{n} lg\frac{(Ni/N)}{(Si/S)} \tag{2}$$

where *Ii* is the information value of a given cell, and *n* is the number of geological factors affecting the cell. The higher the *Ii* value, the greater the possibility of the presence of ore.

3.2. Prediction Variable Selection and 3D Buffer Zones

The Tianpeng Formation, faults (F_3 and secondary faults), granites, and granitic porphyries are closely associated with mineralization in the Bainiuchang ore deposit. The ore bodies mainly occur within the Tianpeng Formation, and mineralization is concentrated in the footwall of F_3, particularly in the contact zones between F_3 and the secondary faults. Granites and granitic porphyries intrude into the mining area, and these intrusions may

have a positive impact on mineralization. The Tianpeng Formation can be divided into three lithological sequences (i.e., $\in_2 t^a$, $\in_2 t^b$, and $\in_2 t^c$ in ascending stratigraphic order), and each sequence is classified as a buffer zone (Figure 5a). We assigned values to the Tianpeng Formation unit cells based on the stratigraphic thickness to obtain the thickness data for the buffer zones (Figure 5b). We searched on both sides of the fault plane to assign the fault buffer zone (F_3 and secondary faults; Figure 5c,d). We searched from the granite or granitic porphyry roof to the outside of the contact zone to assign the granite buffer zone (granites and granitic porphyries; Figure 5e,f).

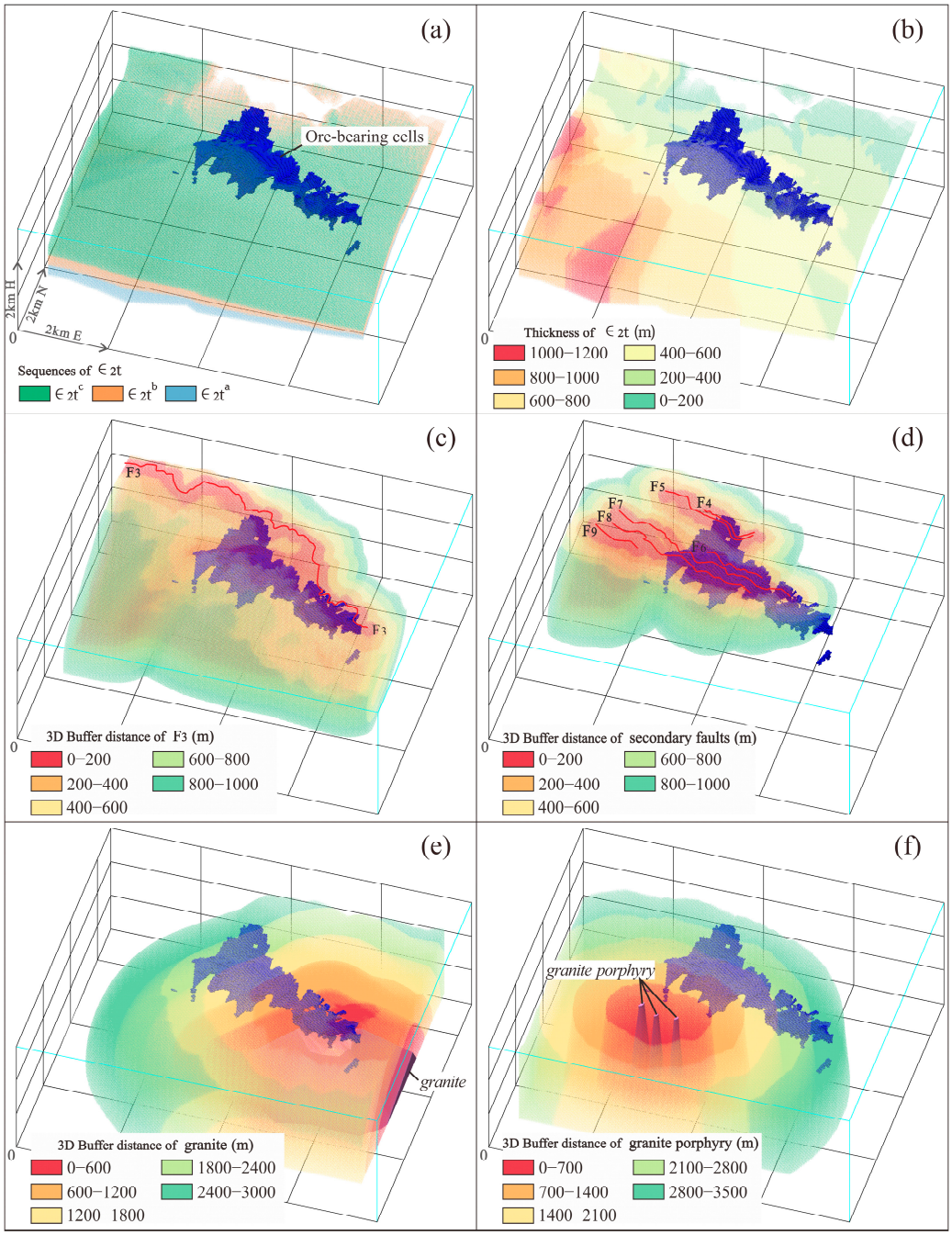


Figure 5. The 3D buffer zones of the ore-controlling geological factors. (**a**,**b**) Buffer zone of the middle Cambrian Tianpeng Formation ($\in_2 t$). (**c**,**d**) Buffer zone of the faults (F_3 and secondary faults). (**e**,**f**) Buffer zone of the granites and granite porphyries.

4. Mineralization Prediction

4.1. Information Value Calculation

The basic statistical distance of buffer zones should be neither too large nor too small. Ideally, the number of ore-bearing cells within adjacent zones should increase or decrease systematically with increasing distance. Based on the buffer zone parameters of each geological factor, the number of cells (Si) and ore-bearing cells (Ni) in each zone were counted, and the values of Si/S and Ni/N in each zone were calculated based on the total number of unit blocks (S = 10,833,067) and ore-bearing cells (N = 25,735). The information values of the geological factors ($I[xi, H]$) in each zone were then calculated (Table 1).

Table 1. Statistical information.

Geological Variables	Distance Interval	Number of Cells in the Zone (*Si*)	Number of ore Cells in the Zone (*Ni*)	*Si*/*S*	*Ni*/*N*	Information Value *I*(*xi*, *H*)	Sort
$\in_2$ t	$\in_2 t^c$	839,830	15,359	0.078	0.597	0.8864	10
	$\in_2 t^b$	895,587	6859	0.083	0.267	0.5084	18
	$\in_2 t^a$	832,884	1337	0.077	0.052	−0.1702	37
Thickness of $\in_2$ t	0–80 m	6942	5	0.0006	0.0002	−0.5183	40
	80–160 m	32,413	422	0.0030	0.0164	0.7388	15
	160–240 m	86,821	1521	0.0080	0.0591	0.8677	11
	240–320 m	122,421	2029	0.0113	0.0788	0.8437	12
	320–400 m	230,732	6415	0.0213	0.2493	1.0683	5
	400–480 m	324,007	6709	0.0299	0.2607	0.9403	9
	480–560 m	271,514	5625	0.0251	0.2186	0.9406	8
	560–640 m	195,065	827	0.0180	0.0321	0.2516	24
F_3	0–20 m	103,076	10,191	0.0095	0.4218	1.6467	1
	20–40 m	126,674	6848	0.0117	0.2835	1.3845	2
	40–60 m	119,777	3108	0.0111	0.1286	1.0658	6
	60–80 m	120,352	1761	0.0111	0.0729	0.8170	13
	80–100 m	121,098	1165	0.0112	0.0482	0.6349	16
	100–120 m	122,199	731	0.0113	0.0303	0.4285	20
	120–140 m	122,850	239	0.0113	0.0099	−0.0593	33
	140–160 m	123,735	116	0.0114	0.0048	−0.3764	39
Secondary faults	0–80 m	203,605	5536	0.0188	0.2291	1.0861	4
	80–160 m	240,655	7330	0.0222	0.3034	1.1354	3
	160–240 m	213,277	4420	0.0197	0.1829	0.9681	7
	240–320 m	233,314	3210	0.0215	0.1329	0.7902	14
	320–400 m	255,572	2089	0.0236	0.0865	0.5641	17
	400–480 m	266,628	684	0.0246	0.0283	0.0608	30
	480–560 m	278,598	532	0.0257	0.0220	−0.0674	34
	560–640 m	293,090	359	0.0271	0.0149	−0.2603	38
Granites	0–300 m	616,985	1541	0.0570	0.0599	0.0218	32
	300–600 m	814,483	3878	0.0752	0.1507	0.3020	23
	600–900 m	941,029	1893	0.0869	0.0736	−0.0722	35
	900–1200 m	1,000,305	3640	0.0923	0.1414	0.1852	27
	1200–1500 m	1,049,528	2804	0.0969	0.1090	0.0510	31
	1500–1800 m	1,005,089	2795	0.0928	0.1086	0.0684	29
	1800–2100 m	907,978	5530	0.0838	0.2149	0.4089	21
	2100–2400 m	758,781	3021	0.0700	0.1174	0.2243	25

Table 1. *Cont.*

Geological Variables	Distance Interval	Number of Cells in the Zone (*Si*)	Number of ore Cells in the Zone (*Ni*)	*Si*/*S*	*Ni*/*N*	Information Value *I*(*xi*, *H*)	Sort
Granite porphyries	0–400 m	460,560	0	0.0425	0.0000	-	-
	400–800 m	657,393	0	0.0607	0.0000	-	-
	800–1200 m	912,176	449	0.0842	0.0174	−0.6836	41
	1200–1600 m	1,166,113	3266	0.1076	0.1269	0.0715	28
	1600–2000 m	1,279,996	7749	0.1182	0.3011	0.4063	22
	2000–2400 m	1,119,395	8372	0.1033	0.3253	0.4981	19
	2400–2800 m	1,022,832	4033	0.0944	0.1567	0.2201	26
	2800–3200 m	1,020,623	1717	0.0942	0.0667	−0.1499	36

The information value represents the strength of the correlation between each prediction variable and the mineralization. In terms of the information values, the top-ranked geological factors were the F_3 fault, secondary faults, and the Tianpeng Formation. The information value for the zone that was 0–60 m from the F_3 fault plane was high. Zones with distances of 0–240 m from the secondary faults were also conducive to mineralization. Zones with a thickness of 320–560 m for the Tianpeng Formation had high information values and were conducive to mineralization. $\in_2 t^c$ was also a favorable location for mineralization.

Positive information values were assigned to the cells in the 3Dmine software system, and each cell had information values related to geological factors such as the Tianpeng Formation, faults, or granites. The total information value of each cell was obtained by summing the information values for each geological factor. A higher total information value indicates a greater possibility of ore occurrence.

A total of 8,953,536 cell information values were obtained, and the maximum, minimum, and mean values were 5.58, 0.02, and 0.70, respectively. The standard deviation was 0.80 and the variance was 0.63. The mean value of the 25,735 ore-bearing cells was 4.00, which was generally higher than that of the other cells. The ore-bearing rate was calculated as the ratio of the number of ore-bearing cells to the total number of cells in an interval (Table 2; Figure 6). The statistical results show that the increase in the information value in each interval with a number of cells tended to decrease (Figure 6a), while the ore-bearing rate tended to increase (Figure 6b). It is possible to reduce the extent of the exploration area based on use of the information values to identify prospecting targets.

Table 2. Information value distribution of the cells in the study area.

Information Value Interval	Number of Cells	Number of Ore-Bearing Cells	Ore-Bearing Rate (%)	Information Value Boundary	Number of Ore-Bearing Cells	Percentage
0.0–0.6	5,873,875	652	0.01	≥0.0	25,735	100.00
0.6–1.2	1,441,356	169	0.01	≥0.6	25,083	97.47
1.2–1.8	801,747	334	0.04	≥1.2	24,914	96.81
1.8–2.4	377,923	553	0.15	≥1.8	24,580	95.51
2.4–3.0	217,822	1739	0.80	≥2.4	24,027	93.36
3.0–3.6	133,292	3794	2.85	≥3.0	22,288	86.61
3.6–4.2	60,247	6002	9.96	≥3.6	18,494	71.86
4.2–4.8	32,122	6211	19.34	≥4.2	12,492	48.54
4.8–5.4	13,644	5764	42.25	≥4.8	6281	24.41
5.4–6.0	1508	517	34.28	≥5.4	517	2.01

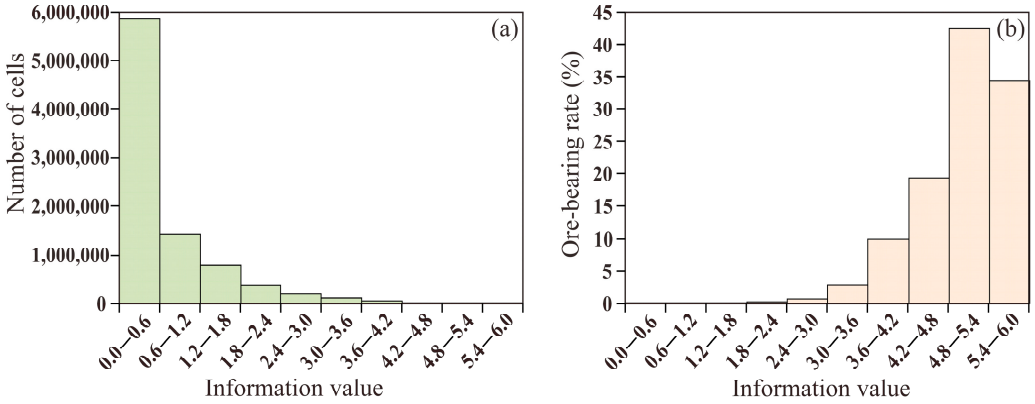


Figure 6. Mineralization prediction based on the weight of evidence method. (**a**) Information values versus the number of cells. (**b**) Information values versus the ore-bearing rate.

4.2. Prediction Boundary of the Total Information Value

We calculated the information value anomaly boundaries using two methods and evaluated these using receiver operating characteristic (ROC) curves to find the best-fit boundaries [24].

The first method counted the number of ore-bearing cells that were larger than the different boundaries and calculated its percentage of the total ore-bearing cells and plots a curve (Table 2; Figure 7a). As the information value boundary increased, the curve changed from flat to steep; and, the boundary information value on the curve was 3.0 (Figure 7a).

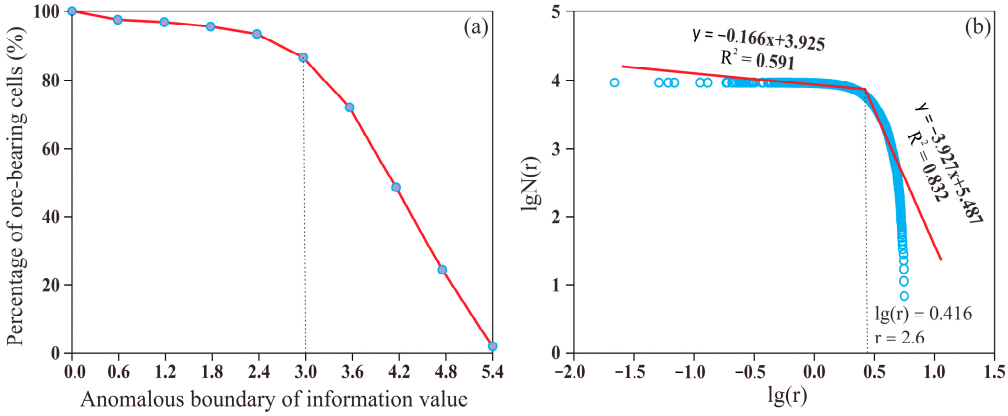


Figure 7. Information value distribution and anomaly boundary calculation curves. (**a**) Anomalous boundary of the information value versus the percentage of ore-bearing cells. (**b**) Information value log–log plot of the cells in the study area.

The fractal approach is an analytical tool based on fractal theory and is widely applied in fields such as geology, geochemistry, and mineral exploration [25–27]. This method is used in geochemical exploration to analyze geochemical background and anomaly threshold values. The second method utilized a 2D fractal approach, whereby an information value log–log plot of the cells was obtained, from which the boundary of the prospecting cells was calculated to be 2.6 (Figure 7b).

The ROC curve was used to evaluate the performance of the prospectivity models [28]. The receiver operating characteristic (ROC) curve is a widely used tool in evaluating the performance of classification models. It plots the true positive rate (sensitivity) against the false positive rate (1-specificity) at various threshold settings. The true positive rate indicates the proportion of actual positives correctly identified by the model, while the false positive rate indicates the proportion of actual negatives incorrectly identified as positives. The area under the ROC curve (AUC) serves as a quantitative measure of model

performance, with values ranging from 0 to 1. A higher AUC value, closer to 1, signifies better model accuracy and performance, indicating a stronger ability to distinguish between classes. Conversely, an AUC value of 0.5 suggests that the model performs no better than random guessing [29]. The ROC curve is particularly useful in fields such as landslide hazard assessment and mineral exploration, where it helps assess the effectiveness of predictive models in classifying different levels of risk or identifying geochemical anomalies associated with mineral deposits.

We used the prediction boundaries of 3.0 and 2.6 as test variables, and whether these belonged to ore-bearing cells as the state variable, to construct the ROC curves (Figure 8). The AUC value of the prediction boundary of 3.0 was 0.791, and that for the boundary of 2.6 was 0.836. However, the 2D fractal method prediction boundary of 2.6 was a better fit.

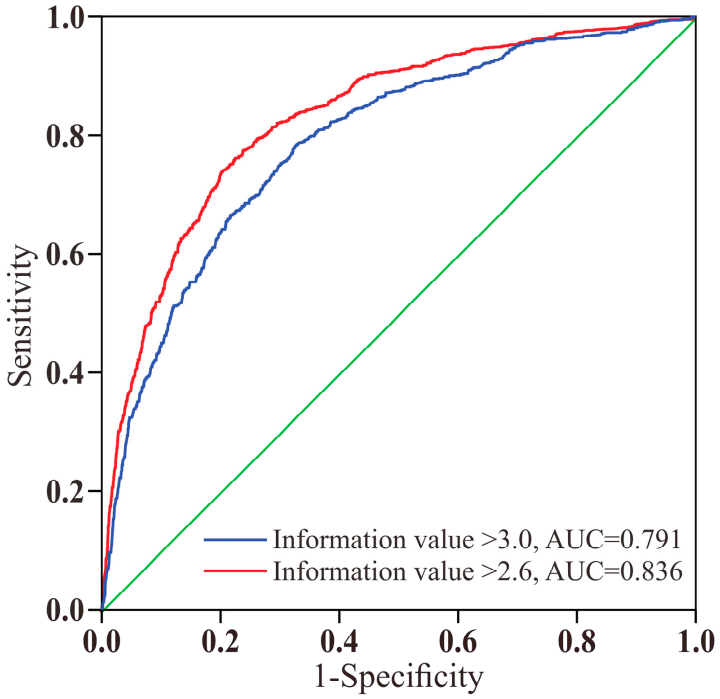


Figure 8. ROC graph for the prediction boundaries.

4.3. Prospecting Target

A total of 376,704 cells were obtained according to the prediction boundary (information value > 2.6), among which 23,561 unit blocks were ore-bearing cells. The mean information value of these was 3.37, and that for the ore-bearing cells was 4.23.

The spatial concentration of anomalous cells at the periphery of the ore bodies and explored areas were selected as the exploration targets. Three target areas were obtained. The A1 target had 28,405 anomalous cells, a volume of 227,240,000 m^3, and a mean information value of 3.35. The A2 target had 59,932 anomalous cells, a volume of 479,456,000 m^3, and a mean information value of 3.03. The A3 target had 19,226 anomalous cells, a volume of 153,808,000 m^3, and a mean information value of 3.41 (Figure 9).

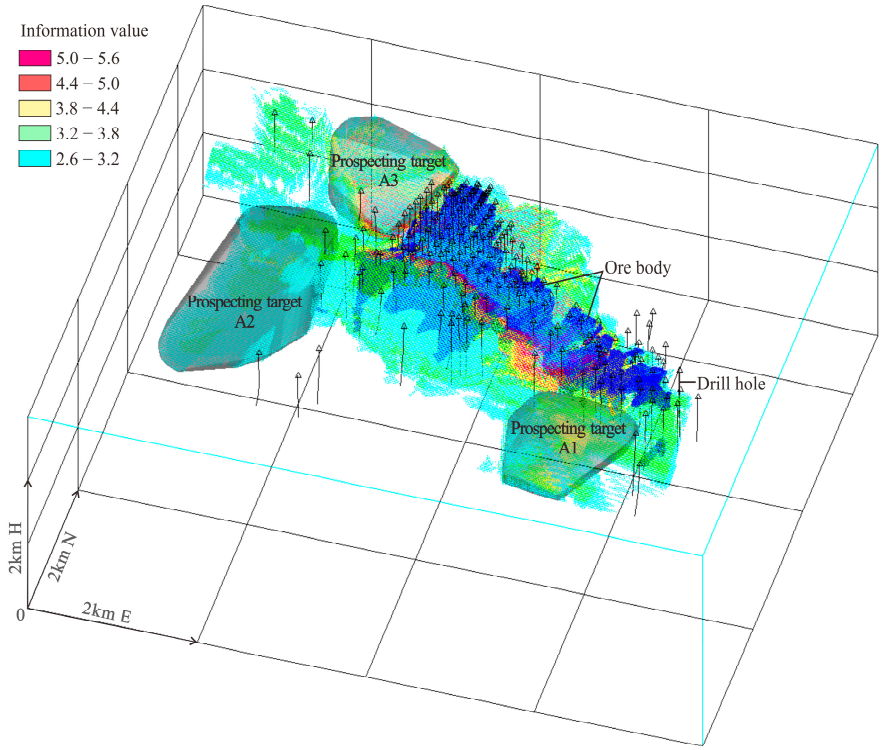


Figure 9. Mineralization prediction map of the study area (information value > 2.6).

5. Results and Discussion

5.1. Ore-Controlling Geological Factors

The origin of the ore materials in the Bainiuchang deposit is debated, with possibilities including a submarine exhalative origin [30], magmatic–hydrothermal origin [31–33], or a combination of both [34,35]. The information value method evaluates the importance ranking of each geological factor for the mineralization prediction based on the spatial relationship between the prediction variables and ore bodies. The top-ranked geological factors were the F_3 fault, secondary faults, and the Tianpeng Formation. The geological factor with the strongest indicative value for mineral prospecting was the F_3 fault. If the deposit was of submarine exhalative origin, there would have been later displacement along the F_3 fault due to differences in physical properties between the ore body and overlying strata. If the deposit was magmatic–hydrothermal in origin, then F_3 may have been the channel for the ore-forming hydrothermal fluids and provided the space for the precipitation of ore materials and the formation of the ore body.

The statistical results showed there was a close spatial relationship between the ore bodies and secondary faults. The ore bodies occurred mainly in the Tianpeng Formation ($\in_2 t^c$), and areas with a thickness of 320–560 m exhibited good mineralization, suggesting that structural and lithological competency controlled the mineralization.

5.2. Information Value Distribution

The statistical results showed that the mean information value of the ore-bearing cells was 4.00, whereas the mean value of all cells was 0.70. A higher information value characterizes a smaller number of cells and is associated with a higher ore-bearing rate (Table 2; Figure 6). This indicated that we can identify prospecting targets based on the total information value.

5.3. Prediction Boundary and Target

The ROC curve evaluation results showed the best prediction boundary of 2.6 (AUC = 0.836) was obtained using the 2D fractal method. Three prospecting targets—A1, A2, and A3—are located in the Tianpeng Formation. A1 is closer to granites in the southeast of the mining area, and the granites may have provided the thermal driving force for the migration of mineralizing fluids. A2 and A3 are spatially related to F_3 and the secondary faults.

6. Conclusions

In this study, a 3D geological model of the Bainiuchang Ag polymetallic deposit was constructed using 3D modeling technology, This model serves as a framework for evaluating geological factors and mineralization potential. The information value method was applied to assess the significance of different geological factors in the mineralization process, revealing that the F_3 fault, secondary faults, and the middle Cambrian Tianpeng Formation are the most critical factors controlling mineralization.

A statistical analysis of the information value distribution revealed that the mean information value of ore-bearing cells was significantly higher (4.00) than that of all cells (0.70). This suggested that areas with higher information values are more likely to contain mineralization. The inverse relationship between the information values and the number of cells indicates that high-value cells are relatively rare, but are associated with a higher ore-bearing rate. This characteristic can be utilized to identify potential exploration targets by focusing on areas with high total information values. This approach can effectively improve the accuracy of mineralization prediction in the study area and optimize exploration efforts.

The ROC curve was used to determine the optimal prediction boundary, which was found to be 2.6 with an AUC value of 0.836 using the 2D fractal method. This boundary effectively distinguishes between areas with high and low mineralization potential. Based on this boundary, three exploration target areas (A1, A2, and A3) were identified within the Tianpeng Formation. These target areas are spatially associated with key geological factors, such as F_3 and the secondary faults. Specifically, A1 is closer to the granite, while A2 and A3 are related to F_3 and the secondary faults. These target areas represent the most promising locations for further exploration and have the potential to yield significant mineral discoveries.

The modeling results have important implications for the Bainiuchang and other similar deposits. They can be used to guide deep and peripheral exploration activities, helping to identify new mineralization zones and expanding the resource base. The integration of 3D geological modeling and the information value method demonstrates that this approach is robust and effective for mineralization prediction. This approach can be adapted and applied to other mineral deposits with similar geological settings, providing a valuable tool for the exploration industry to enhance the efficiency and success of mineral exploration.

This study offers valuable insights into the mineralization potential of the Bainiuchang deposit, it is crucial to recognize certain limitations, particularly regarding the data and model assumptions. The 3D geological model was constructed based on existing geological data, which may be subject to spatial limitations and uncertainties. The information value method assumes that the spatial relationships between geological factors and mineralization are consistent throughout the study area. Future research will focus on validating these assumptions with additional data, such as geophysical and geochemical exploration data, and refine the mineralization prediction framework.

Author Contributions: Methodology, F.J., J.G., G.Z. and H.C.; formal analysis, F.J., G.M., L.J., P.P., Z.W. and C.Y.; investigation, F.J., L.J., H.C. and P.P.; resources, F.J., G.Z., G.M. and L.J.; data curation, F.J., Z.W. and C.Y.; writing—original draft preparation, F.J.; funding acquisition, G.Z., J.G. and H.C.; All authors have read and agreed to the published version of the manuscript.

Funding: This research was funded by a Research Fund Project of the Yunnan Provincial Department of Education (Grant 2025J1389), the Doctoral Research Start-up Fund of Kunming Metallurgy College in 2021 (Grant Xxrcxm202102), and a Yunnan Provincial Major Science and Technology Special Program Project (Grant 202402AB080006).

Data Availability Statement: The original contributions presented in this study are included in the article. Further inquiries can be directed to the corresponding author.

Acknowledgments: We thank Jiaxi Zhou of Yunnan University for their valuable suggestions.

Conflicts of Interest: The authors declare that the research was conducted without any commercial or financial relationships that could be perceived as potential conflicts of interest.

References

1. Chen, J.P.; Shi, R.; Chen, Z.P.; Wang, L.M.; Sun, Y. 3D positional and quantitative prediction of the Xiaoqinling gold ore belt in Tongguan, Shaanxi, China. *Acta Geol. Sin.* **2012**, *86*, 653–660. [CrossRef]
2. Li, X.H.; Yuan, F.; Zhang, M.M.; Jia, C.; Jowitt, S.M.; Ord, A.; Zheng, T.K.; Hu, X.Y.; Li, Y. Three-dimensional mineral prospectivity modeling for targeting of concealed mineralization within the Zhonggu iron orefield, Ningwu Basin, China. *Ore Geol. Rev.* **2015**, *71*, 633–654. [CrossRef]
3. Mohammadpour, M.; Bahroudi, A.; Abedi, M. Three dimensional mineral prospectivity modeling by evidential belief functions, a case study from kahang porphyry cu deposit. *J. Afr. Earth Sci.* **2021**, *174*, 104098. [CrossRef]
4. Li, C.; Liu, B.L.; Xiao, K.Y.; Kong, Y.H.; Wang, L.; Tang, R.; Xie, M.; Wu, Y.X. Metallogenic Prediction of the Zaozigou Gold Deposit Using 3D Geological and Geochemical Modeling. *Minerals* **2023**, *13*, 1205. [CrossRef]
5. Payne, C.E.; Cunningham, F.; Peters, K.J.; Nielsen, S.; Puccioni, E.; Wildman, C.; Partington, G.A. From 2D to 3D: Prospectivity modelling in the Taupo Volcanic Zone, New Zealand. *Ore Geol. Rev.* **2014**, *71*, 558–577. [CrossRef]
6. Nielsen, S.H.H.; Cunningham, F.; Hay, R.; Partington, G.; Stokes, M. 3D prospectivity modelling of orogenic gold in the Marymia Inlier, Western Australia. *Ore Geol. Rev.* **2015**, *71*, 578–591. [CrossRef]
7. Mao, X.C.; Zhang, B.; Deng, H.; Zou, Y.H.; Chen, J. Three-dimensional morphological analysis method for geologic bodies and its parallel implementation. *Comput. Geosci.* **2016**, *96*, 11–22. [CrossRef]
8. Huang, J.X.; Deng, H.; Mao, X.C.; Chen, G.H.; Yu, S.Y.; Liu, Z.K. 3D modeling of detachment faults in the Jiaodong gold province, eastern China: A Bayesian inference perspective and its exploration implications. *Ore Geol. Rev.* **2023**, *154*, 105307. [CrossRef]
9. Porwal, A.; Carranza, E.J.M. Introduction to the Special Issue: GIS-based mineral potential modelling and geological data analyses for mineral exploration. *Ore Geol. Rev.* **2015**, *71*, 477–483. [CrossRef]
10. Roshanravan, B.; Aghajani, H.; Yousefi, M.; Kreuzer, O. An improved prediction-area plot for prospectivity analysis of mineral deposits. *Nat. Resour. Res.* **2019**, *28*, 1089–1105. [CrossRef]
11. Mao, X.C.; Ren, J.; Liu, Z.K.; Chen, J.; Tang, L.; Deng, H.; Bayless, R.C.; Yang, B.; Wang, M.J.; Liu, C.M. Three-dimensional prospectivity modeling of the Jiaojia-type gold deposit, Jiaodong Peninsula, Eastern China: A case study of the Dayingezhuang deposit. *J. Geochem. Explor.* **2019**, *203*, 27–44. [CrossRef]
12. Xiao, K.Y.; Xiang, J.; Fan, M.J.; Xu, Y. 3D mineral prospectivity mapping based on deep metallogenic prediction theory: A case study of the Lala Copper Mine, Sichuan, China. *J. Earth Sci.* **2021**, *32*, 348–357. [CrossRef]
13. Zhang, Q.P.; Chen, J.P.; Xu, H.; Jia, Y.L.; Chen, X.W.; Jia, Z.; Liu, H. Three-dimensional mineral prospectivity mapping by XGBoost modeling: A case study of the Lannigou gold deposit, China. *Nat. Resour. Res.* **2022**, *31*, 1135–1156. [CrossRef]
14. Zhang, H.P.; Liu, J.S.; Li, X.B.; Zhang, X.L. Relationship of granites to tin, silver, copper, lead, zinc, polymetallic deposits in southeastern Yunnan China. *Contrib. Geol. Miner. Resour. Res.* **2006**, *21*, 87–90.
15. Du, S.J.; Wen, H.J.; Liu, S.R.; Qin, C.J.; Yan, Y.F.; Yang, G.S.; Feng, P.Y. Mineralogy and Metallogenesis of the Sanbao Mn–Ag (Zn-Pb) Deposit in the Laojunshan Ore District, SE Yunnan Province, China. *Minerals* **2020**, *10*, 650. [CrossRef]
16. Wang, Q.; Li, J.W.; Jian, P.; Zhao, Z.H.; Xiong, X.L.; Bao, Z.W.; Xu, J.F.; Li, C.F.; Ma, J.L. Alkaline syenites in eastern Cathaysia (South China): Link to Permian–Triassic transtension. Earth Planet. *Sci. Lett.* **2005**, *230*, 339–354. [CrossRef]
17. Yang, G.S.; Wang, K.; Yan, Y.F.; Jia, F.J.; Li, P.Y.; Mao, Z.B.; Zhou, Y. Genesis of the ore-bearing skarns in Laojunshan Sn-W-Zn-In polymetallic ore district, southeastern Yunnan Province, China. *Acta Petrol. Sinica.* **2019**, *35*, 3333–3354. [CrossRef]

18. Luo, J.H.; Zhao, Z.L.; Li, W.; Huang, L.; Zhao, W.Q. Landslide hazard assessment of an urban agglomeration in central Guizhou Province based on an information value method and SVM, bagging, DNN algorithm. *Sci. Rep.* **2025**, *15*, 2483. [CrossRef] [PubMed]
19. Fagbohun, B.J.; Aladejana, O.O.; Okonye, I.F.; Tobore, A.O. Assessing gully erosion susceptibility dynamics using information value and hazard index methods: A case study of Agulu-Nanka watershed, Southeast Nigeria. *Catena* **2024**, *241*, 108070. [CrossRef]
20. Chen, Y.F.; Chen, L.W.; Peng, Z.H.; Zhang, M.; Hu, Y.S.; Oua, Q.H.; Zhang, J.; Tian, Y.; Shi, X.P. An improved model to predict the water-inrush risk under an unconsolidated confined aquifer based on analytic hierarchy process and information value method. *Geomat. Nat. Hazards Risk* **2023**, *14*, 2236277. [CrossRef]
21. Cao, J.S.; Qin, S.W.; Yao, J.Y.; Zhang, C.B.; Liu, G.D.; Zhao, Y.Y.; Zhang, R.C. Debris flow susceptibility assessment based on information value and machine learning coupling method: From the perspective of sustainable development. *Environ. Sci. Pollut. Res.* **2023**, *30*, 87500–87516. [CrossRef] [PubMed]
22. Yin, K.L. Statistical prediction model for slope instability of metamorphosed rocks. In Proceedings of the 5th International Symposium on Landslides, Lausanne, Switzerland, 10–15 July 1988; Volume 2, pp. 1269–1272.
23. Zêzere, J.L. Landslide susceptibility assessment considering landslide typology, a case study in the area north of Lisbon (Portugal). *Nat. Hazards Earth Syst. Sci.* **2002**, *2*, 73–82. [CrossRef]
24. Hanley, J.A.; Mcneil, B.J. A method of comparing the areas under receiver operating characteristic curves derived from the same cases. *Radiology* **1983**, *148*, 839–843. [CrossRef] [PubMed]
25. Zhao, M.Y.; Xia, Q.L.; Li, W.J. Identifying geochemical element distribution patterns through multiple-point geostatistical simulation and singularity analysis: A case study of the Wulonggou-Balong Area, Qinghai, China. *Geochemistry* **2025**, *85*, 126294. [CrossRef]
26. Sharifi, M.; Rajabzadeh, M.A.; Peace, A.L. Analysis of Spatial Association of Mineralization and Faults Through Fry and Fractal Modelling in Anarak Metallogenic Zone, Iran. *Iran. J. Sci.* **2025**, *49*, 65–77. [CrossRef]
27. Fils, S.C.N.; Mongo, C.H.B.; Mimba, M.E.; Mboua, A.C.C.; Bassahak, J.; Nouck, P.N.; Hell, J.V. Spatial distribution and characteristics of lineaments using fractal and multifractal analysis for evaluating the structural controls on a regional-scale gold mineralization, Cameroon, Central Africa. *J. Geovisualization Spat. Anal.* **2024**, *8*, 21. [CrossRef]
28. Yang, N.; Zhang, Z.K.; Yang, J.H.; Hong, Z.L. Applications of data augmentation in mineral prospectivity prediction based on convolutional neural networks. *Comput. Geosci.* **2022**, *161*, 105075. [CrossRef]
29. Fawcett, T. An introduction to ROC analysis. *Pattern Recognit. Lett.* **2006**, *27*, 861–874. [CrossRef]
30. Zhu, C.H.; Zhang, Q.; He, Y.L. The characteristics of mineralizing elements of the Bainiuchang silver Polymetallic deposit in southeastern Yunnan. *Bull. Mineral. Petrol. Geochem.* **2005**, *24*, 327–332.
31. Liu, J.S.; Zhang, H.P.; Fang, W.X.; Guo, J.; Zhang, X.L. Problems pertaining to Bainiuchang silver, polymetallic deposit in Mengzi country Yunan China. *Strateg. Study CAE* **2005**, *7*, 238–244.
32. Zhang, Y.H.; Zhang, S.T.; Liu, H.W. A Comparative Study on Ore- Controlling Factors of Large- Scale Polymetallic Ore Deposits in Bozhushan Area of Southeast Yunnan. *J. Kunming Univ. Sci. Technol. (Sci. Technol.)* **2012**, *37*, 1–7.
33. Li, K.W.; Zhang, Q.; Wang, D.P.; Cai, Y.; Liu, Y.P. LA-ICP-MS U-Pb zircon dating of the Bozhushan granite in Southeast Yunnan. *Chin. J. Geochem.* **2013**, *32*, 170–180. [CrossRef]
34. Chen, X.C.; Hu, R.Z.; Bi, X.W.; Zhong, H.; Lan, J.B.; Zhao, C.H.; Zhu, J.J. Zircon U–Pb ages and Hf–O isotopes, and whole-rock Sr–Nd isotopes of the Bozhushan granite, Yunnan province, SW China: Constraints on petrogenesis and tectonic setting. *J. Asian Earth Sci.* **2015**, *99*, 57–71. [CrossRef]
35. Jian, L. Superimposed Mineralization System and Metallogenic Model of Bainiuchang Super Large Polymetallic Deposits, Southeastern Yunnan, China. Ph.D. Dissertation, Kunming University of Science and Technology, Kunming, China, 2016.

Disclaimer/Publisher's Note: The statements, opinions and data contained in all publications are solely those of the individual author(s) and contributor(s) and not of MDPI and/or the editor(s). MDPI and/or the editor(s) disclaim responsibility for any injury to people or property resulting from any ideas, methods, instructions or products referred to in the content.